Developments in fluorescence lifetime-based analysis for ultra-HTS

Sandra Turconi, Ryan P. Bingham, Ulrich Haupts and Andrew J. Pope

Homogeneous fluorescence detection methods are proving key in the establishment of miniaturized ultra-HTS (uHTS). Fluorescence lifetime-based methods seem set to provide an additional dimension to these approaches and are likely to represent a significant further advance both in terms of increasing measurement robustness and in opening up completely new types of uHTS assay format.

Sandra Turconi*, Ryan P. Bingham, Ulrich Haupts and Andrew J. Pope
GlaxoSmithKline Pharmaceuticals,
New Frontiers Science Park (north), Third Avenue
Harlow, UK CM23 5HE
*tel: +44 1279 627592
fax: +44 1279 627599
e-mail: sandra_turconi-1@gsk.com

▼ Fluorescence techniques are now widely applied in HTS and their continued application and development is a major underpinning for the realization of uHTS [defined as $>10^5$ assay day^{-1} in a working volume of ≤10 µl and using high density (i.e. ≥1536-well) assay plates] as a robust, routine process[1–3]. A major advantage of fluorescence techniques compared with more conventional formats (e.g. radioisotope-based methods), is that they provide highly-sensitive measurements of fluorophore environment, which enables construction of miniaturized assays with no separation steps[2]. One disadvantage of fluorescence methods is that artefacts caused by signal background, which originate from sample carriers, biological reagents and, most importantly in a uHTS context, from test compounds, can be significant[4]. Various discriminating fluorescence techniques, such as FA (see Box 1 for abbreviations) (Ref. 4), TRET (Refs 5–7), and confocal fluctuation methods such as FCS (Refs 8–10) and FIDA (Refs 11,12), reduce this problem using various means[1,2].

One attractive alternative approach to extracting the true analyte signal from the background fluorescence, is to measure the (characteristic) lifetime of the fluorescent signal of interest. Moreover, if fluorescence lifetimes originating from labelled biomolecules could be reliably determined within the constraints of uHTS, a whole new set of approaches to homogeneous biological assays would be opened up in which lifetime changes provide the primary assay readout. However, until very recently, measurements of fluorophore lifetime required relatively specialized, expensive and low-throughput equipment, which was not suited to HTS and/or uHTS. These instruments are based on two different detection principles of fluorescence lifetime: time domain and frequency domain measurements. A third method that takes advantage of lifetime changes is based on gated detection. The latter is known as TRET or HTRF (Refs 6,7,13, 14), and has been successfully applied in a number of high-throughput screens[15–20]. Recent hardware developments now enable testing the use of direct lifetime measurements using the two distinct measuring principles, both of which are potentially compatible with HTS and/or uHTS. We therefore start this article with a short introduction to fluorescence lifetime and lifetime measurement techniques, and then demonstrate the HTS and/or uHTS applicability of the different approaches with data on biological systems obtained recently in our laboratory. For a more detailed explanation of fluorescence theory, see texts by Lakowicz[21,22].

Fluorescence lifetime

Fluorescence emission is a cyclic process in which fluorophores repeatedly absorb excitation light to form an excited state (typically on the fsec timescale), which decays, via emission of a fluorescence photon, back to the ground state ready for re-excitation. Fluorescence lifetime (τ_f) is defined by the average time the molecule spends in the excited

1359-6446/01/$ – see front matter PII: S1471-1931(01)00159-8

DDT Vol. 6, No. 12 (Suppl.), 2001

state before returning to the ground state and, for most fluorophores, is of the order of nsec. Lifetime is therefore determined by the rate of loss of the excited state, which can occur either by fluorescence emission (at rate Γ) or by other non-radiative competing processes (collectively represented by rate k_{nr}).

$$\tau_f = 1/(\Gamma + \Sigma k_{nr}) \quad (1)$$

The competition with other de-excitation processes depends on the electronic structure of the fluorophore and its interaction with the environment. Non-radiative decay of the excited state can occur via many mechanisms, such as inter-system crossing (ISC, resulting in formation of a triplet state), collisional or static quenching (k_q), solvent effects and resonance energy transfer (k_{ET}), all of which can influence τ_f (Fig. 1a). Often, subtle environmental, electronic and conformational effects alter τ_f observed for fluorophores when attached to bio-active molecules as they participate in their normal reactions (e.g. when bound to a specific binding site compared to free in solution).

The quantum efficiency (ϕ) of a fluorophore is the ratio between absorbed photons and emitted fluorescence photons, and corresponds to the proportion of de-excitation via fluorescence emission. It can therefore also be defined in terms of the rate constants of the different processes leading to de-excitation:

$$\phi = \Gamma/(\Gamma + \Sigma k_{nr}) \quad (2)$$

Quantum yield and lifetime are therefore directly related. The product of ϕ and the molecular absorption coefficient ε (i.e. the capacity of the molecule to capture photons) can be taken as a measure of the molecular brightness, *q*, of the fluorophore, which describes how many photons a fluorophore emits at a given excitation intensity. A change in molecular brightness, as induced, for example, by a binding process, results in a change in total fluorescence intensity. Molecular brightness can be determined as a specific molecular quantity by FIDA (Ref. 2). In addition, Eqn (2) suggests that it will be accompanied by a change in lifetime as well (as changes of ε are unlikely). Fluorescence intensity is a composite property that is dependent on the exact amount and concentration of the probe present and the instrument set up. It is, therefore, sensitive to small variations in pipetted volume as well to interference from compounds, plates and scattered light. Hence, a small signal change could easily be masked by these interferences, preventing a robust assay. By contrast, fluorescence lifetime is an intrinsic property, independent of probe volume, concentration and instrument setup. Therefore, lifetime is measurable in relatively precise terms, given appropriate instrumentation.

Importantly, in FRET, donor lifetime changes in direct relation to donor emission intensity. The donor emission is limited by energy transfer efficiency E and can be described by Eqns (3)–(5):

Box 1. Abbreviations

APC	Allophycocyanin
Bt	Biotin
cFLA	Confocal fluorescence lifetime analysis
FA	Fluorescence anisotropy
FCS	Fluorescence correlation spectroscopy
FD	Frequency domain
FI	Fluorescence intensity
FIDA	Fluorescence intensity distribution analysis
FLARe	Fluorescence lifetime analysis repertoire
FOR	Fair Oaks red
FRET	Fluorescence resonance energy transfer
GPCR	G-protein-coupled receptor
HTRF	Homogeneous time-resolved fluorescence
LDI	Lifetime discriminated intensity
LDL	Lifetime discriminated lifetime
LDP	Lifetime discriminated polarization
LED	Light emitting diode
MLC	Metal-ligand complexes
SA	Streptavidin
TD	Time domain
TRET	Time-resolved energy transfer

$$E = R_0^6/(R_0^6 + r^6) \quad (3)$$

$$E = 1 - (I_{da}/I_d) \quad (4)$$

$$E = 1 - (\tau_{da}/\tau_d) \quad (5)$$

where R_0 is the distance for half energy transfer; r is the distance separating the donor and acceptor; I_{da} and I_d are the intensities of the donor in the presence and absence of acceptor, respectively; and τ_{da} and τ_d are the lifetimes of the donor in the presence and absence of acceptor. Consequently, the change in intensity induced by FRET should be exactly mirrored by a change in lifetime (because $I_{da}/I_d = \tau_{da}/\tau_d$). Therefore, FRET measurements can be performed directly by measurement of the effect upon donor lifetime.

Time-gated fluorescence measurements

In homogeneous HTS assays, a discrimination between sample signal and background fluorescence based on different lifetimes, has currently only been realized in the special case of TRET (Refs 5,13,14) measurements. This technique makes use of lanthanide complexes, which exhibit extremely long-lived (τ_f ~1–2 msec) emission resulting from forbidden transitions between 5d and 7f orbitals. In this case, the analyte (Ln^{3+} complex) shows an emission lifetime of approx 10^5 times longer than that of background signals, which typically exhibit lifetimes of <10 nsec. Therefore, simple time-gated detection of the output signal following flash illumination enables effective suppression of short-lived background signals (Fig. 1b). A typical flash-measure cycle has a

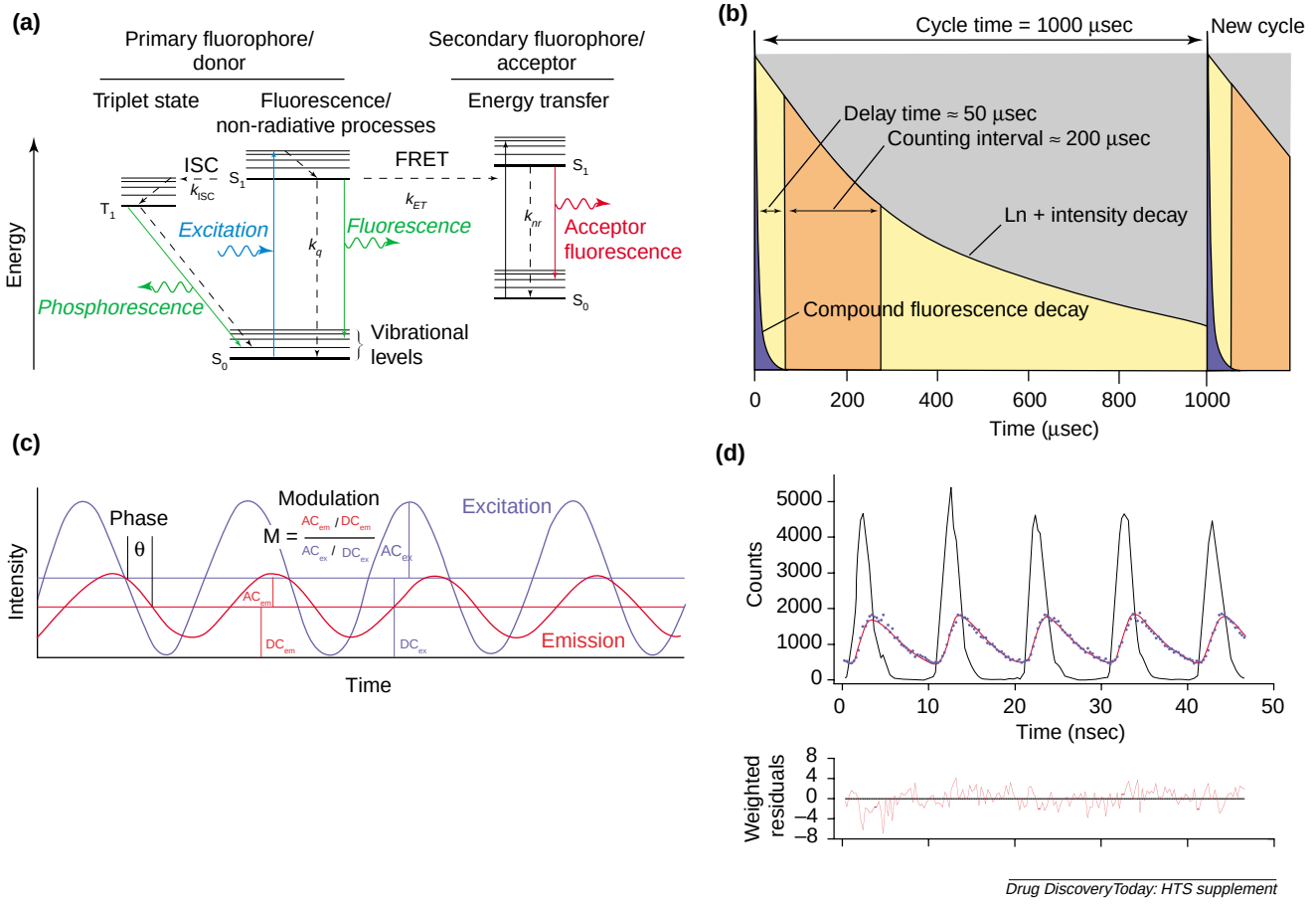

Figure 1. (a) Jablonski diagram illustrating the main processes governing the properties of fluorescence emission. The dotted lines represent non-radiative (nr) processes. (b) The principle of time-gated experiments. (c) The principle of the frequency-modulation method for measurement of fluorescence lifetimes. The blue line indicates modulated excitation light (ex) and the red line indicates emitted fluorescence (em). M is the modulation ratio, composed of the AC (alternate current) and DC (direct current) components of the photomultiplier signal. (d) The principle of single-photon counting technique. The top graph shows experimental data (blue) and fit (red) against the pulse-train profile. The bottom graph is a plot of weighted residuals (deviations of the data from the theoretically fitted function) used for the fit quality control. Abbreviations: ISC, inter-system crossing; q, quenching; ET, energy transfer; S_0 and S_1, singlet ground and excited states, T_1, excited triplet state.

duration of ~1 msec, enabling many repeats (e.g 10^3) during the measurement of each sample. This time-gated measurement scheme, coupled with the use of fluorescent Ln^{3+} chelates[13] or cryptates[14] and suitable resonance energy acceptors, has been successfully applied in a number of HTS assays[15–20]. In every case, the principle behind the assays is a change of Ln^{3+} emission lifetime via changes in resonance energy transfer as the proximity of donor and acceptor change during the reaction being studied. As a result, the amount of Ln^{3+} emission detected in a given time window (typically 50–250 µsec) decreases with increasing energy transfer, while acceptor emission increases.

However, TRET systems are not without their problems. First, lanthanide complexes are excited in the UV light range, where absorbance owing to test compound and biological matrices reduces signal level caused by the inner-filter effect. Second, the actual measured parameter is the fluorescence intensity within the pre-determined time-window, rather than the more-reliable lifetime change. For this reason, all TRET systems employ internal correction schemes (yet can still be prone to interference)[15], and have relatively tight boundary constraints on the conditions used in order to achieve robust signals. The reason for this is the limit imposed by the measurement time window (Fig. 1b), which partly reflects, but does not in any way analytically describe, the lifetime profile observed when the Ln^{3+} tracer is in proximity to or distant from the acceptor fluorophore. In addition, TRET assays require relatively specialized and expensive reagents, as well as labelling of two reaction partners.

The hardware systems used for TRET measurements do not approach the time-resolution that would be required in order to make such measurements using conventional 'prompt'

fluorophores (where τ_f <10 nsec), nor do they permit direct determination of τ_f for those systems with suitably long lifetimes (e.g. Ln^{3+} complexes). Here, we describe results obtained using two new HTS and/or uHTS compatible systems, in which τ_f is a directly determined output parameter and where the usable fluorophore lifetime range is extended downwards to, in the case of one of the approaches, the direct measurement of τ_f in fluorophore systems in common use.

Both approaches make use of the basic methodology that has been applied in expensive and low-throughput research grade instruments for a number of years and, indeed, currently provide the basis to determine fluorophore lifetimes within a research setting. These techniques are distinguished by the nature of the excitation/emission cycles utilized and are referred to in general terms as time domain (TD) and frequency domain (FD) methods[21,22].

FD-lifetime measurements

In FD measurements, the intensity of the excitation light is sinusoidally modulated with a certain frequency (Fig. 1c). Upon excitation of a fluorescent molecule with such a modulated light, the emitted fluorescence will also be modulated. However, the modulation depth (peak-to-trough height) will be decreased, and the phase will be shifted in the emitted light. This phase and modulation change is directly related to and is used to calculate the lifetime based on Eqn (6):

$$\omega\tau = \tan\theta = (1/M^2 - 1)^{1/2} \qquad (6)$$

where ω is the angular modulation frequency (2π times modulation frequency); τ is the lifetime; θ is the phase; and M is modulation[23]. To recover the fluorescence decay parameters from the signal response of the emission, a non-linear least-square fitting procedure is performed, as described in Ref. 21.

The phase shift and decrease of modulation depth become noticeable when ω is roughly 1/100 of the decay rate Γ of the fluorophore, and approach their maximum ($\pi/2$ phase shift and complete demodulation) at $\omega > 10 > \Gamma$. The modulation frequency at which the phase shift and demodulation are most sensitive to changes of the tracer lifetime is about 1/5 of Γ. If the lifetime of the tracer is around 300–400 nsec and the short-lived background fluorescence is $\tau = 5$ nsec (and therefore $\omega < 1/100\ \Gamma_{bk}$), the contribution of the background fluorescence to the phase shift and demodulation is negligible at this point. This forms the basis of background discrimination in screening applications[24,25].

Another advantage of this approach is the non-pulsed nature of the light source. This means that relatively high light intensities can be achieved, resulting in the sample being illuminated almost as efficiently as in normal (continuous lamp) FI experiments. By contrast, in time-domain set-ups the sample is mostly 'in the dark'.

FD measurements in HTS – FLARe

The FLARe system is a prototype system capable of performing frequency domain-based lifetime measurements in 96- or 384-well microtitre plates and developed by Molecular Devices (Sunnyvale, CA, USA)[25,26] (formerly LJL BioSystems). The principal aims of the development of the FLARe system were to exploit the ability of lifetime-discriminated measurements to exclude spurious background signals. By exciting a long-lifetime fluorescent tracer with light modulated at a frequency matched to its lifetime, fluorescence emissions of a markedly different lifetime are suppressed. This background discrimination can be applied to either fluorescence intensity signal (LDI) or to fluorescence anisotropy (LDP). However, an obvious pre-requisite for this approach to be successful is that the background emission should have a markedly different lifetime to that of the tracer fluorophore. Background signals from, for example, autofluorescence, have lifetimes in the low-nanosecond range and therefore tend to overlap directly in terms of lifetime with commonly used 'prompt' fluorophores, such as fluorescein, rhodamine and cyanine dyes. FLARe therefore provides no advantage when using such tracers (where τ_f <10 nsec), and is also unsuitable for use with very long lifetime Ln^{3+} systems as modulated LED systems used for excitation are so far only available down to ~370 nm, compared with an excitation maxima of <340 nm.

For this reason, a specific set of intermediate lifetime probes is required in order to gain benefits from the lifetime-discrimination abilities of FLARe. One example of these are the transition MLCs (Ref. 21). These compounds display molecular fluorescence from a metal-to-ligand charge transfer state. This transition is partially forbidden* and, as a result, fluorescence decay times are long[27]. In the case of ruthenium (Ru)-MLCs (supplied as probes for FLARe by Molecular Devices), lifetimes are around 350 nsec (Ref. 25) and therefore very well separated from that of normal background autofluorescence. In addition, these dyes have large Stokes shifts, with excitation maximum at 467 nm and a broad emission centred at 605 nm.

Of particular interest in the context of the potential use of this approach for HTS and/or uHTS, is the extent to which the FLARe technique can compensate for or ameliorate interferences caused by test library compounds. This was examined using a model assay system based upon Bt–SA binding. This very high affinity interaction (K_d ~10^{-15} M) was ideal for testing the robustness of new assay readout strategies to the presence of test matrices, because it is, essentially, refractory to all compounds in our collection (and in any case, assays established using nanomolar reagent concentrations are at ~$10^6 \times K_d$, and therefore require very high affinity

*Some electronic transitions are forbidden or partially forbidden according to electronic configuration and symmetry rules. Transition processes still take place, but their statistical probability is lower. This is reflected in lower rate of such processes.

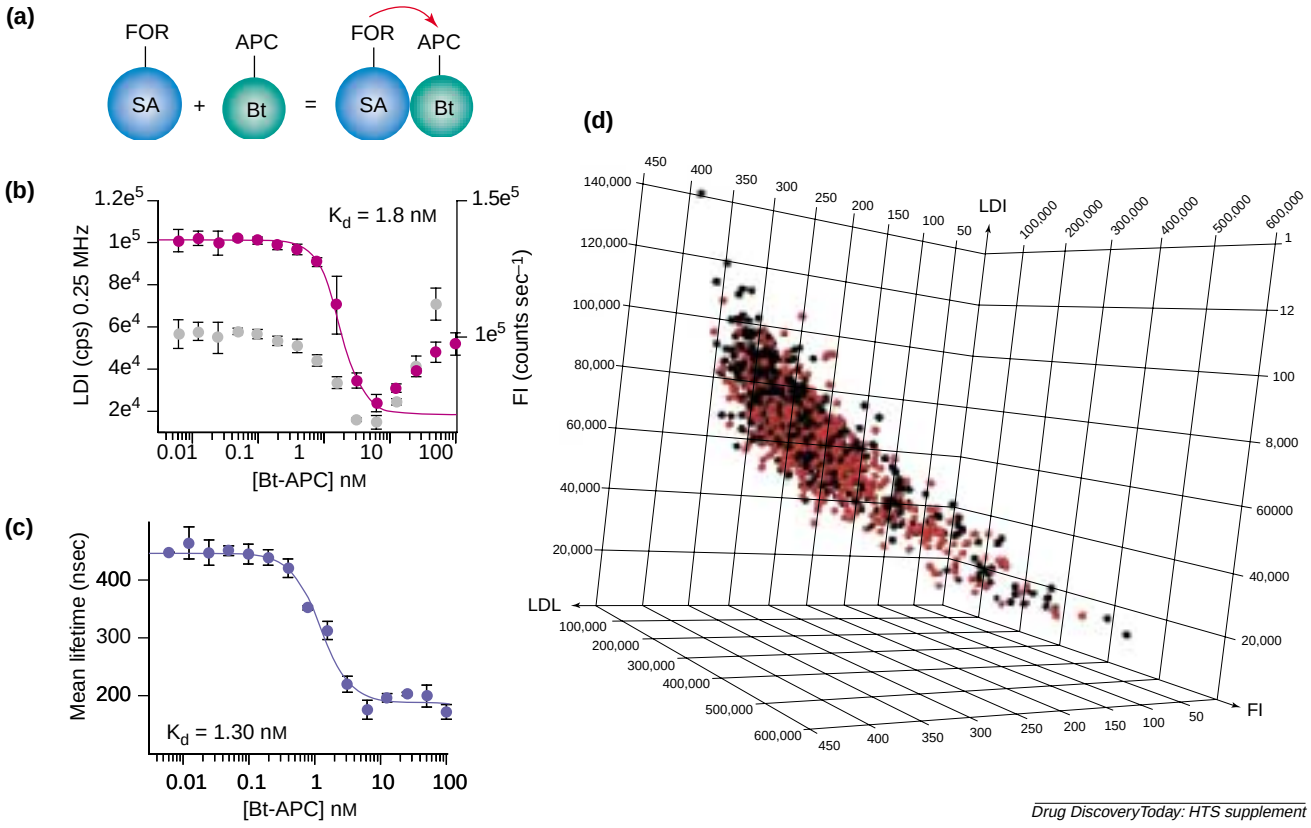

Figure 2. Use of FLARe to ameliorate compound interferences in FOR–APC FRET assays. (a) The FRET-based FOR-SA–Bt-APC model assay system. (b) Changes in LDI (magenta) and FI (grey) fluorescence. $K_{d,app}$ = 1.8 nM (limited by [ligand] and fitted disregarding the data above 10 nM APC owing to APC autofluorescence). (c) Mean lifetime (blue) upon binding of Bt-APC to FOR-SA (20 nM). $K_{d,app}$ = 1.3 nM. (d) Effect of test compounds on FI, LDI and LDL signal from 1408 single (black) or mixture (red) test compound wells. All measurements were performed with a modulation frequency of 0.25 MHz. For abbreviations, see Box 1.

compounds in order to produce competitive displacement). SA was labelled with the Ru-complex FOR (LJL BioSystems), and bound to a Bt-APC conjugate obtained commercially (Europa Bioproducts, Cambridge, UK) (Fig. 2a). As would be predicted from the spectral overlap of FOR with APC, formation of the SA-FOR–Bt-APC complex led to a measurable reduction in both FOR intensity and mean lifetime by FRET (450–200 nsec), as measured by the FLARe system (Fig. 2b,c). The increase of the LDI signal at Bt-APC concentrations above 10 nM is caused by the the strong sensitized fluorescence from APC, which is clearly not fully suppressed by lifetime-discrimination. The total fluorescence intensity trace is given in the same figure for comparison.

Maximum background suppression is obtained in FLARe when the excitation light is modulated with a frequency matched to the tracer fluorophore lifetime (in this case FOR), yielding a maximum LDI signal/background (and an approx five-fold change during the APC-Bt–SA-FOR binding interaction). This stems from the basic relationship between fluorophore lifetime and frequency as shown in Eqn (6). However, more-complex equations are needed to describe mixtures of fluorophores[24,25]. The potential benefits of using the LDI signal should become clear when the effect of test compounds on this or non-discriminated intensity is examined. A set of test compounds was assayed either as discrete single samples (10 μM of each compound) or pooled mixtures of eight compounds (12.5 μM of each compound) at 20 nM SA-FOR and 5 nM Bt-APC. This compound selection was random and not based on optical or any other properties of the compounds. FI, LDI and LDL were all measured for FOR emission at 605 nm. The comparison and relationship of these parameters is best viewed in 3D space (Fig. 2d). As expected, the FOR intensity values showed very large amounts of scatter in the presence of test compounds. Most of this scatter is towards high FI values, indicating that the cause of this scatter is autofluorescence of the compounds. The use of the LDI and LDL parameter was expected essentially to eliminate this scatter. However, the wells that showed high FI values gave low values for both LDI and LDL. This effect can be seen in the 3D graph as the combined data produced an almost perfect diagonal

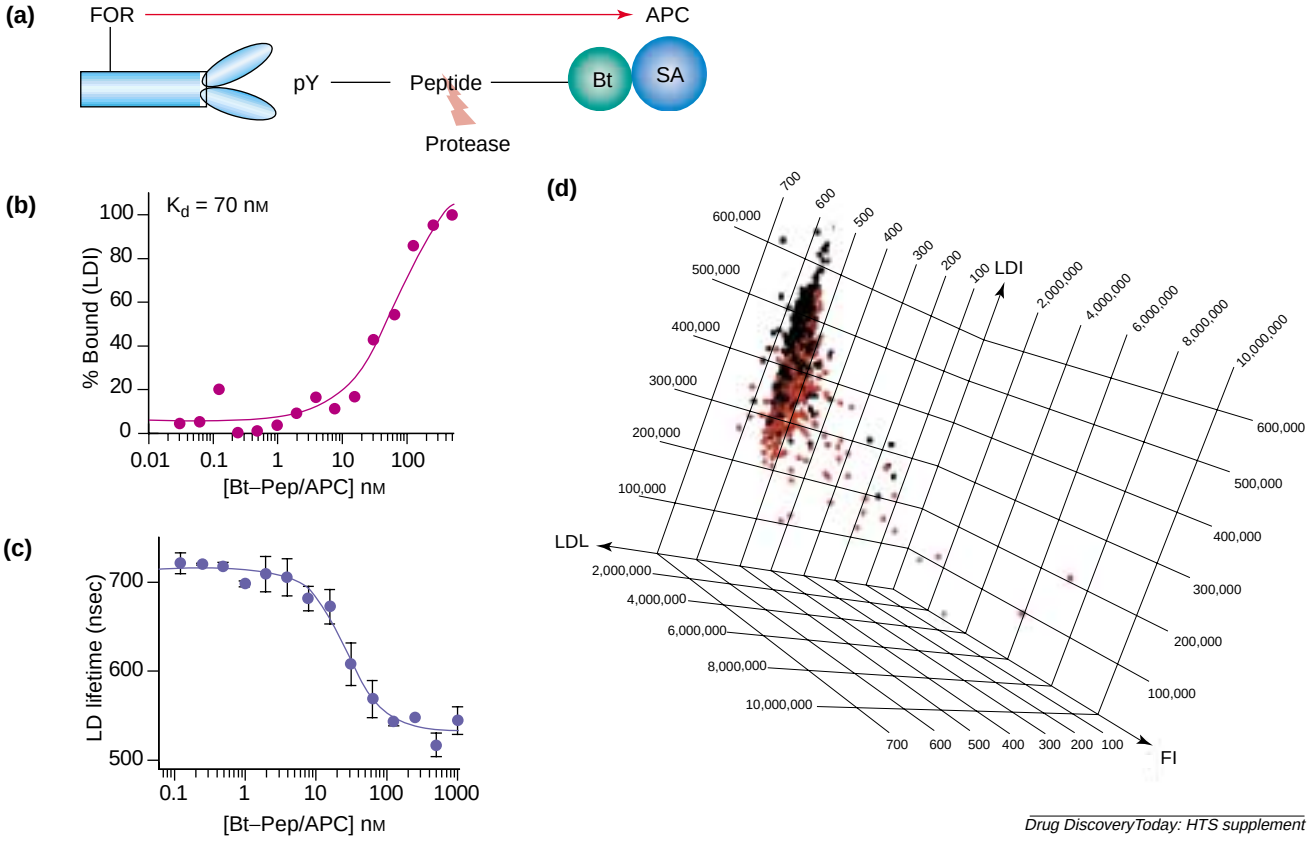

Figure 3. Use of FLARe to ameliorate compound interferences in FOR–APC FRET assays. **(a)** FRET-based protease assay system. The light-blue structure is an anti-phosphotyrosine (pY) antibody. **(b)** Changes in LDI (expressed in % bound peptide) and **(c)** lifetime upon titration of the biotinylated peptide (and SA–APC, 1:1 ratio) into 10 nM FOR-anti-pY. K_d = 70 nM. **(d)** Effect of test compounds on FI, LDI and LDL signal from 1408 single (black) or mixture (red) test compound wells. All measurements were performed with a modulation frequency of 0.25 MHz. For abbreviations, see Box 1.

in the 3D cube. Therefore, all the output parameters are colligative and do not yield an improvement in signal robustness.

It is important that these data are placed in an appropriate context because not all simple intensity-based fluorescence measurements produce such poor results in the presence of test compounds. The crucial factor is the relative signal contributions obtained from the tracer of interest compared with the background signal from test compounds. In fact, FOR and other Ru-based fluorophores are relatively dim and when used at 40 nM (with a labelling ratio of two FOR per SA) as shown in Fig. 2, produce a marginal intensity signal, particularly when compounds are present. Under these circumstances, LDI certainly results in real improvements. However, when using more conventional prompt fluorophores that produce a much more intense fluorescence, there is normally far less of a problem. In practice, the way in which conventional fluorescence intensity assays are configured is to use an appropriate tracer concentration where it is known that a robust signal (over the real background in the presence of autofluorescent test compounds rather than buffer blanks) is obtained.

An additional complication of using the Ru charge-transfer probes required for FLARe measurements, is that the conjugation chemistry is less straightforward than when using more conventional fluorophores. Nevertheless, we and others have successfully developed FLARe-based assays for relevant therapeutic targets[28]. Fig. 3a shows the format of one such assay for protease activity based upon FRET between FOR and APC positioned on either side of a protease cleavage site within a synthetic peptide substrate. The FRET decreases FOR FI and lifetime (Fig. 3b,c). Upon proteolytic cleavage, these changes are reversed. The effect of the same set of test compounds as used against the SA–Bt model system on the FI, LDI and LDL is shown in 3D in Fig. 3d. The results show some similarities with the SA–Bt assay in FI and LDI readouts – the wells displaying high FI also display low LDI. However, the LDL shows a clearly narrower distribution of values compared with the other two parameters. The lifetime is also significantly longer in this system (720 nsec compared to 450 nsec in the SA–Bt system described above), which certainly influences the effectiveness of discrimination. Therefore, LDL would be the detection parameter of choice for a screen in this

particular case. Nevertheless, 22 wells of pooled mixtures showed LDL values below low control (500 nsec). Furthermore, although the concentration of the FOR label was comparable in these two examples, the FOR FI signal was five-fold higher in the protease assay. This is caused by the diminished efficiency of energy transfer owing to a significantly increased distance between FOR (donor) and APC (acceptor). The spacing introduced by the 16-amino-acid peptide could be up to 8 nm (in extended conformation), which is close to the R_0 for this FRET pair (6.1 nm) (Chen, J. *et al.* Fluorescence-lifetime reagents for sensitive and robust assays. Poster presented at the *Annual Meeting of the Society for Biomolecular Screening*, 6–9th September 2000, Vancouver, BC, Canada). As the energy-transfer-efficiency-dependence on distance is a very steep function around the R_0 value [$1/R_0^6$ (see Eqn 3)], such changes in donor emission efficiency are to be expected.

In cases where Ru charge-transfer dyes such as FOR are used in assays, the FLARe system provides some limited improvements in the signal robustness, obtained in the presence of test compound libraries. This was observed only for the second assay system investigated owing to better background discrimination achieved through increased FOR FI and fluorescence lifetime. A further crucial question is when the use of such dyes would be preferred over more conventional organic fluorophores, such as cyanine dyes. One circumstance might be in the use of lifetime-discriminated anisotropy assays. The long lifetime of the Ru dyes (or any others that would be of utility in FLARe) means that fluorescence is depolarized in higher molecular weight complexes relative to that of the dyes normally used for anisotropy experiments[1]. This could potentially open up new applications for anisotropy, such as protein–protein interactions or chemokine–GPCR binding assays. However, these are still largely unexplored and it is not known whether dyes such as FOR provide sufficient brightness for use in such measurements under useful boundary conditions (i.e. achievable concentration of reagents in relation to K_d)[12]. During our assessment of the FLARe system, a considerable effort was undertaken to identify alternate probes such as fluorophores with lifetime >20 nsec, which would have utility in FLARe. However, we were unable to find any other suitable probes for the system (G. Chan and S. Turconi, unpublished results).

TD-based lifetime measurements

In contrast to frequency-domain techniques, time-domain methods are based on a pulsed source of excitation light. The fluorescence is triggered by a train of light pulses illuminating the sample. In traditional single photon counting set-ups, the pulses are spaced such that the fluorescence provoked by a pulse can decay completely before the next pulse starts. However, one can also work at shorter spacing and de-convolute the signal taking into account the overlap of decay curves[21]. The time delay between the excitation pulse and the detection of the fluorescence photon is measured for a large number of pulses (Fig. 1d). Histograms are constructed from this data representing the number of photons (y-axis) detected at a certain time after the excitation (x-axis). This histogram defines the fluorescence decay, which in turn is fitted with a (multi) exponential model using a non-linear least squares fit algorithm[29]. The parameters derived are fluorescence lifetime(s), and respective amplitudes (fractional contributions), in case more than one fluorescence process contributes to the decay. With short fluorescence lifetimes, the light source can be pulsed at quite high rates (e.g. 100 MHz), enabling a very large number of measurements to be performed in a very short time. The result is a fluorescence decay accumulated over approx 10^5 events (0.5 sec $well^{-1}$, 200 kHz counting rate) with very high signal-to-noise ratios. Lifetimes can therefore be determined with very high precision, and even small changes in lifetime are detected reliably. The achievable time-resolution is determined by the response profile of the system and the width of the time segments (bins) in the detection electronics.

TD-lifetime measurements in uHTS – cFLA

Fluorescence lifetime detection in confocal volume has been reported[30] and implemented in a prototype DNA-sequencing instrument[31]. Confocal detection methods have recently been implemented in an HTS and/or uHTS compatible form by Evotec Biosystems (Hamburg, Germany) and cFLA is the most recent addition to this family. Apart from the underlying technique used to de-convolute analyte fluorescence lifetime, it is also important to recognize that these methods are distinguished from FLARe in the fundamental optical setup used. The FLARe system uses a modified fluorescence plate reader in which macroscopic fluorescence signals are measured, that is, the signal is averaged over a volume that is a significant proportion of the sample volume itself. In this case, signal amplitude and signal-to-background ratios are sensitive to both sample volume and concentration. By contrast, the cFLA technique uses diffraction-limited confocal optics in which the detection volume is a tiny proportion of the sample carrier (1 fl). In this case, the signal output is essentially independent of assay volume and exhibits little background contribution compared with conventional macroscopic readers. This property, which is shared with other microscopic methods such as FCS (Refs 2,8) and FIDA (Refs 2,11), makes these techniques well suited to miniaturized uHTS. The potential advantages of these approaches have been well-documented[2]. As FIDA and FCS are fluctuation-based single-molecule methods, the tracer concentration has to be in the nanomolar range, resulting in, on average, just a few molecules (<10) in the confocal volume. It is important to point out that this restriction does not apply to cFLA because it is not a fluctuation-based method and a wide range of tracer concentrations (sub-nanomolar to millimolar) is possible. As the lifetime of interfering compounds can be expected to be of

similar magnitude to the tracer lifetime (1–10 nsec), it is also important to point out that the cFLA does not provide an inherent method of discriminating between tracer and compound interference as is the case with FLARe and FIDA (Refs 1,2). However, at the long wavelength applied in these tests (635 nm), much less interference can be expected compared with shorter wavelengths that are commonly used (488 nm, 543 nm).

The prototype cFLA instrument is based on an inverted Zeiss microscope equipped with a 40×, 1.15 NA water immersion objective. The beam of a pulsed laser diode (635 nm, 100 MHz) is fed into the instrument through a back port and the confocal volume imaged through a 70 μm pinhole onto an avalanche photo diode. Photon detection in the cFLA instrument is based on the well-known time-correlated single-photon timing technique in which a detected fluorescence photon starts an electronic clock, which is stopped by the following laser pulse. The pulse distance minus the measured time yields the time delay for the particular photon[29]. Both instruments discussed here can perform measurements in 96-well plates. However, cFLA is capable of utilizing a 2080-well plate with 1 μl well-volume, whereas the FLARe uses low-density plates (384-well) in a volume of 10 μl. cFLA requires glass-bottom plates.

Unfortunately, the cFLA and FLARe systems we have tested use mutually exclusive excitation wavelengths (FLARe uses 475 nm and 535 nm modulated LED sources, whereas cFLA uses a 635 nm pulsed laser diode) and time ranges (FLARe needs tracers with lifetimes >200 nsec, whereas cFLA was designed for use with prompt dyes with lifetimes of <5 nsec). Direct comparison of these systems using the same set of dyes is therefore not possible.

In cFLA, the lifetime or intensity amplitudes of the fluorescent tracer in a mixture of different lifetime components is measured (in contrast to the lifetime-discriminated measurements performed on FLARe). Therefore, changes in lifetime of the fluorescent tracer are a pre-requisite of cFLA assays. However, a number of mechanisms exist for modulation of lifetime change, as already described. The two most important mechanisms utilized to date are FRET (where the change in donor lifetime is a direct measure of FRET efficiency), or conformational/environmental effects on a single tracer dye. In principle, the latter provide a much simpler approach because only a single label is required. However, it is difficult to predict *a priori* whether such effects are likely to occur for any given system in contrast to other fluorescence techniques in which the design of assay formats is highly predictive[1].

Because effects upon tracer conjugate brightness that occur during biological reactions (e.g. labelled-ligand binding to its receptor) can cause distortions and artefacts in techniques such as FA and FCS (Refs 1,8), we have tended in the past to concentrate upon systems in which such changes are minimized. Therefore, a new set of probes could be required for cFLA techniques. An example of this can be found in the cyanine dyes. Recently, in our laboratories, the use of Cy3™ in FA assays has largely been replaced by its rigid counterpart, Cy3B™. Cy3B is around three-fold brighter than Cy3, presumably owing to the elimination of rotational isomerization of the polyene system by the introduction of additional bridging ring structures. In the unrestricted Cy3 molecule, the excited state can decay via the radiationless mechanism of isomerization around the double bond. This process accounts for the reduced quantum efficiency when compared with Cy3B and appears as dark state formation on the microsecond time-scale in FCS-type experiments. Interestingly, we have observed in a number of systems that this process tends to be reduced when conjugates labelled with Cy3 or its longer wavelength analogue, Cy5™, are bound to their biological receptors, presumably via torsional constraints imposed upon the bound form. This strongly suggests that Cy3 and Cy5 might exhibit changes in lifetime under these circumstances. This dye was focussed on initially as Cy5 is compatible with the 635 nm excitation source available on the prototype cFLA system. However, we have also examined a number of other dyes excited at 635 nm (Table 1) by synthesizing conjugates for a number of biological systems. These could be rapidly characterized as potential probes for cFLA simply by examining the fluorescence intensities observed for free and bound tracer-conjugate forms. In each case, the affinity and specificity of the reaction could be readily confirmed using conventional techniques such as FA or FCS.

As with FLARe, the robustness of cFLA signals to test compounds was a crucial factor, and this was examined using a Bt–SA model. In this case, the construction of the assay was extremely simple: Bt was labelled with Cy5 (Cy5-Bt) and mixed with SA. Binding of Cy5-Bt to SA resulted in a lengthening of the Cy5 lifetimes from 0.9 nsec (the same as free Cy5) to 1.45 nsec (Fig. 4a,b). Conventional FA measurement confirmed that the FI measurement showed a concomitant 2.3-fold intensity increase upon binding.

The titration of SA resulted in a pronounced lifetime-change and enabled the construction of the binding curve shown in Fig. 4b. The determined value of $K_{d,app}$ of 0.9 nM is limited by the tracer concentration, as the Bt–SA interaction is of much higher affinity. The robustness of the signal change can be quantified in terms of the so-called Z′ value[32]. A Z′ value of >0.5 is usually considered acceptable. To mimic the typical signal that would be used in a screening assay, subsequent measurements were made at an SA concentration of $1.7 \times K_{d,app}$ (1.5 nM, highs) versus free Cy5-Bt (lows). Z′ values obtained as a function of different read-times for this system are given in Fig. 4c. Good Z′ values were obtained even for very short measuring times. The Cy5-Bt–SA model system was also tested against the same set of test compounds as used to examine the robustness of FLARe (Fig. 4d). For test compounds present as singles, the distribution of average lifetime values is very tight: a total of six outliers were found (defined as values outside the average $\pm 3 \times$ SD). Pooled mixtures of eight compounds

Table 1. Properties of some commercially available dyes for fluorescence-lifetime applications

Dye	Structure	Supplier	Maximum absorbance (nm)	Maximum emission (nm)	ϵ (mol^{-1} cm^{-1})	Fluorescence lifetime (nsec)	Comments
Cy5	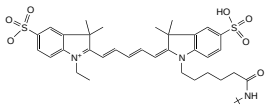	Amersham Pharmacia Biotech[a]	649	670	250,000	0.8	Lifetime increases to 1.1–1.2 nsec upon conjugation
MR121	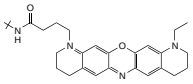	Roche[b]	660	674	n.a.	1.7	
MR200	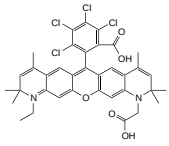	Roche[b]	620	640	75,000	3.5	
DY-630	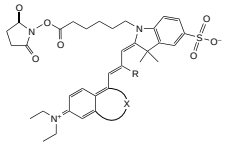	Dyomics[c]	621	652	n.a.	0.2	Lifetime increases upon coupling to nucleotides (2.2 nsec) and proteins (2.6 nsec)
DY-635	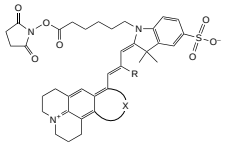	Dyomics[c]	634	664	200,000	0.4	Lifetime increases upon coupling to nucleotides (1.7 nsec) and proteins (2.6 nsec)
Alexa 633	n.a.	Molecular Probes[d]	632	647	80,000	3.2	Lifetime decreases to 2.5 nsec upon conjugation
Bodipy 630/650	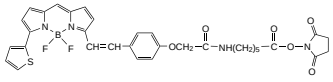	Molecular Probes[d]	625	640	100,000	4.1	
Bodipy 650/670	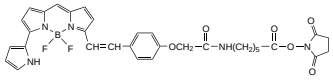	Molecular Probes[d]	646	660	100,000	2.7	
Evoblue	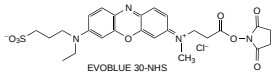	Evotec Biosystems[e]	650	670	100,000	0.9	
Fair Oaks Red	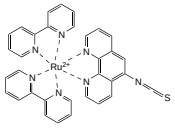	Molecular Devices[f]	467	607	n.a.	361	Ruthenium–CT complex for LDI applications
Sunnyvale Red	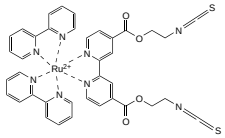	Molecular Devices[f]	488	670	n.a.	360	Ruthenium–CT complex for LDP (fundamental anisotropy 0.28)

[a]Little Chalfont, UK.
[b]Penzberg, Germany.
[c]Jena, Germany.
[d]Leiden, The Netherlands.
[e]Hamburg, Germany.
[f]Sunnyvale, CA, USA.
Abbreviations and explanations: n.a., not available; CT, charge transfer; LDI, lifetime discriminated intensity; LDP, lifetime discriminated polarization. ϵ is the standard symbol for extinction coefficient.

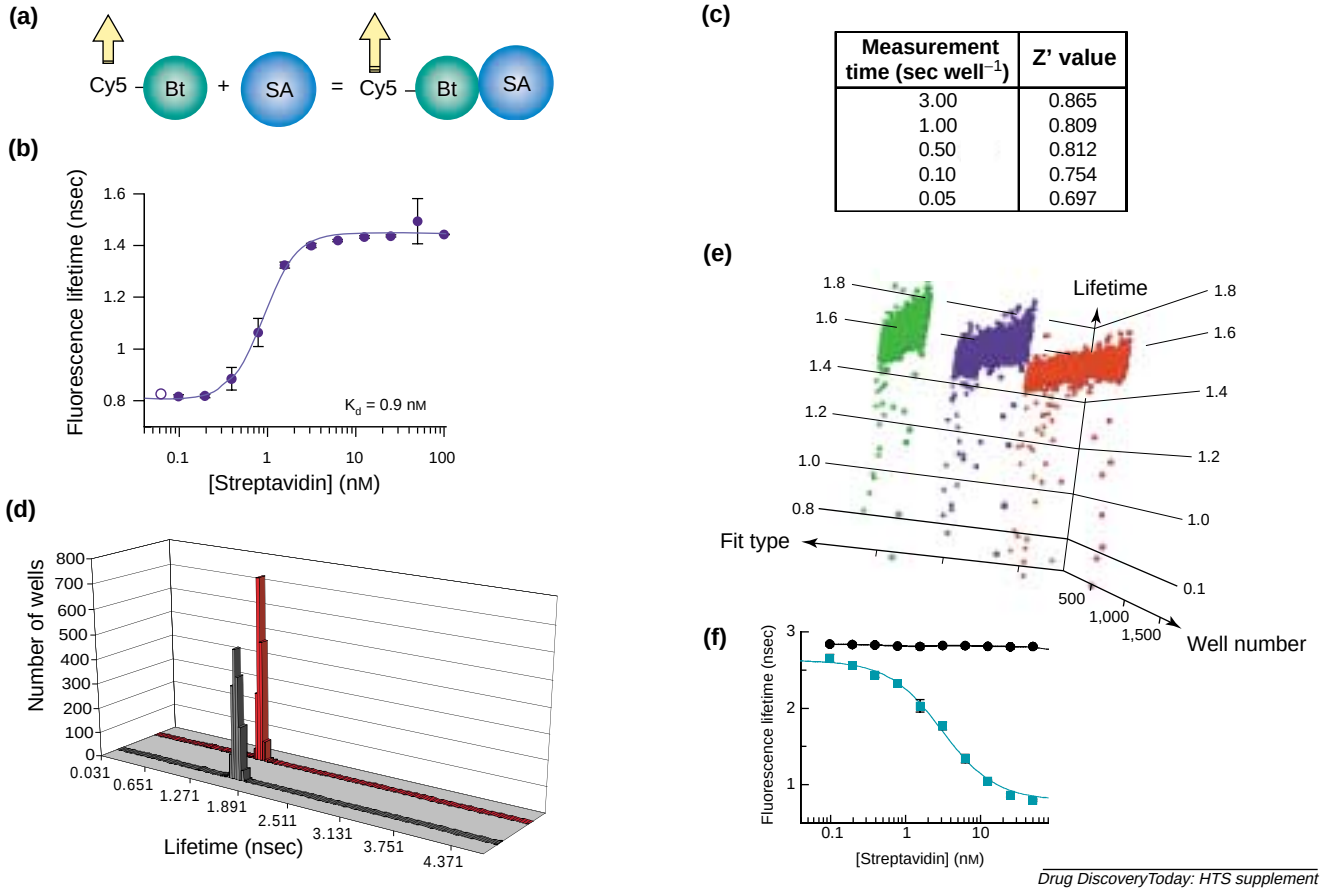

Measurement time (sec well^{-1})	Z' value
3.00	0.865
1.00	0.809
0.50	0.812
0.10	0.754
0.05	0.697

Figure 4. Bt–SA interaction as a model assay for testing the cFLA technique. **(a)** The assay scheme. **(b)** Binding curve generated by titration of SA into 5 nM Cy5-Bt. $K_{d,app}$ = 0.9 nM. **(c)** Z′ values for >30 wells, each of low controls (i.e. background, 5 nM Cy5-Bt only) or highs (signal level at 5 nM Cy5-Bt + 1.5 nM SA) at different measuring times per well. Highs–lows define the 'data window'. **(d)** Lifetime signal distribution for single compounds (grey) and pooled mixtures (red) at 5 nM Cy5-Bt and 1 nM SA; **(e)** Comparison of the signal distribution for pooled mixtures [data set as in (d)], fitted with either a single exponential single lifetime (red) or a constant scatterer component (blue), and two lifetimes (one fixed at 0.4 nsec, green). The difference in chi-square (quality of the fit) was less than 5% for these different models. **(f)** Titration of unlabelled streptavidin (black) or Alexa-660-streptavidin (teal) into 5nM biotin-Alexa633. The fluorescence lifetime of Alexa-633 changes owing to energy transfer to Alexa660 upon binding. For abbreviations, see Box 1.

gave a somewhat more complex picture, with a higher scatter of lifetime values (26 outliers). However, the distribution of lifetime values is still narrow compared with conventional macroscopic fluorescence techniques (Fig. 5e shows FI signals of the same compound set). All of the histograms shown in this figure are directly comparable as they were constructed with each bin being 2% of the average value, and the total range being 2 × the average.

For the pooled mixtures, a total of 28 wells showed a decrease in lifetime (potential hits). However, 12 wells gave a lifetime below the control (free Cy5-Bt) value. This is almost half the number of such 'problem' wells found in FLARe. The source of such a large decrease in lifetime can be either short-lived background fluorescence or scattered light. These are common causes of 'compound interference' in most fluorescence detection approaches and not characteristic of lifetime measurements. Four of these wells showed increased fluorescence intensity (>1.5 × the average), indicating the shorter overall lifetime is most likely owing to a short-lived fluorescence from autofluorescent compounds. The remaining eight wells show average intensities and the most likely cause of this downward trend of fluorescence-lifetime values is scattered light, which effectively has zero lifetime. The data in the above experiments were fitted with only one lifetime component (in case of other interfering processes), resulting in average values. In further analysis, the mixture dataset was fitted to either a monoexponential decay with an additional light-scatter component (lifetime = 0, amplitude fitted only), or to a bi-exponential decay, with the second lifetime component being fixed at different values in the range 0.1–0.5 nsec. These latter two showed reduced scatter in the main (free-fitting) lifetime value (Fig. 4e). The number of

wells showing lifetimes below the low control level has been reduced to five for mono-exponential fit plus scatter, and to only two for the bi-exponential fit. Thus, unlike conventional FI or FA assays, the effect of background fluorescence and scattered light can be minimized in fluorescence lifetime assays.

This performance was confirmed using a more realistic target in a binding assay for inhibitors of bacterial methionyl-tRNA synthetase (MRS) (Fig. 5a). A high-affinity inhibitor of this enzyme was labelled with Cy5, and upon binding of this ligand an increase in the fluorescence lifetime of the Cy5 fluorophore was observed as before. This enabled the determination of the affinity of the ligand of $K_d = 7$ nM (Fig. 5b). The specificity of interaction and its use in a competitor-type assay are exemplified by the displacement experiment shown in Fig. 5c. The Z′ values for read times of 3.0, 1.0, or 0.5 sec well^{-1} were all above 0.8, indicating a very robust assay, although the signal change might appear small; 0.35 nsec, or 30% of the lifetime of the free ligand. The MRS concentration of 12.5 nM ($1.8 \times K_d$) was chosen for the displacement experiment and for the screen against the selection of compounds, as in previous examples. These experiments were performed at read-times of 0.5 and 1.0 sec well^{-1} with practically identical data quality. The signal distributions over 1408 wells, each containing single compounds or compound mixtures, are shown in Fig. 5d. Again, the signal distribution is tight for single compounds (13 outliers), but somewhat less so for mixtures (31 outliers). The four mixture wells that showed lifetimes below the low control level were disregarded. To compare this signal distribution to a conventional read-out, the same compound selection (both singles and mixtures) was read in conventional FI, against 10 nM Cy5-Bt (compared with 5 nM in the cFLA experiments). The signal distribution given in Fig. 5e shows the comparison to cFLA. The histograms were constructed such that the range and the width of the bins are proportional to the signal average. Therefore, the distributions can be compared directly. It is clear that cFLA gives a much narrower signal distribution at a lower tracer concentration. Moreover, the cFLA data are characterized by high reproducibility. This is owing to electronic binning of the signal and to the high repetition rates that enable collection of thousands of decays within very short experimental read-times.

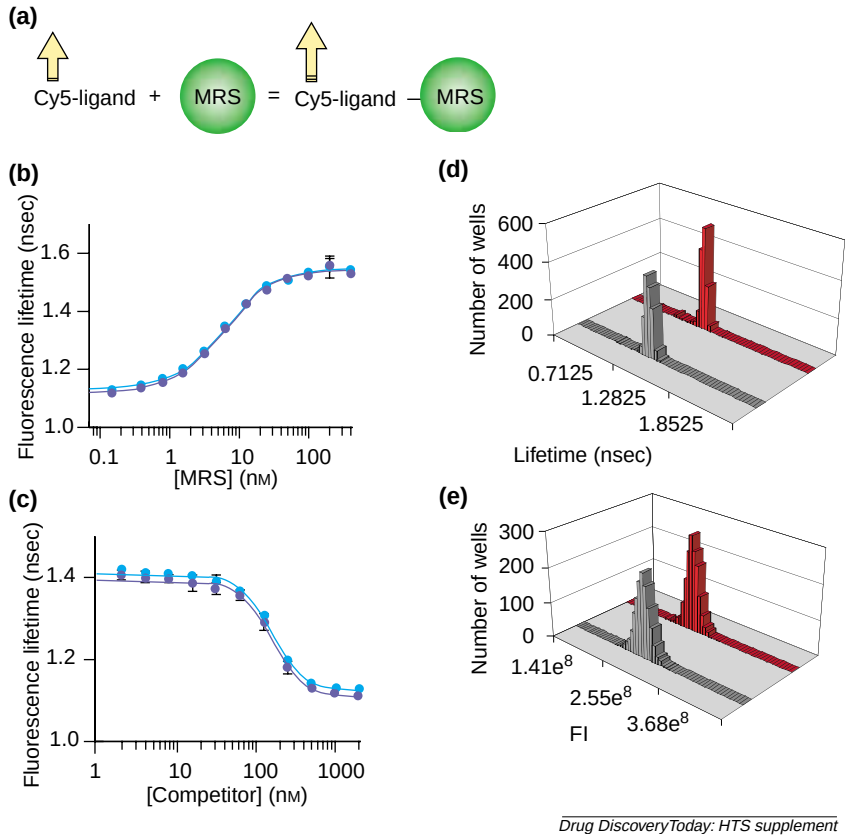

Figure 5. Methionyl-tRNA Synthetase (MRS) interaction with a Cy5-labelled inhibitor: an assay system for testing the cFLA technique. **(a)** The assay scheme. **(b)** Binding curve generated by titration of MRS into 5 nM Cy5-ligand. $K_d = 7$ nM. The purple and blue lines indicate measurements taken at 1 sec well^{-1} and 0.5 sec well^{-1}, respectively. **(c)** Displacement curve at 12.5 nM MRS and 5 nM Cy5-ligand, mimicking the action of an inhibitor. $K_d = 55$ nM. The purple and blue lines indicate measurements taken at 1 sec well^{-1} and 0.5 sec well^{-1}, respectively. **(d)** Fluorescence lifetime signal distribution over 1408 wells containing either single compounds (grey) or pooled mixtures (red) at 12.5 nM MRS and 5 nM Cy5-ligand. **(e)** Fluorescence intensity signal distribution for 10 nM Cy5-Bt. Experiment was setup as (d), with single compounds (grey) or pooled mixtures (red). For abbreviations, see Box 1.

The assays described so far have relied on fluorescence-lifetime change induced by changes in the environment of the fluorophore upon binding. However, lifetime changes induced by energy transfer is another potentially useful assay format. This is demonstrated in Fig. 4f. Here, Bt was labelled with the Alexa-633 dye (Molecular Probes, Leiden, The Netherlands). Upon binding to SA, no lifetime change was observed. However, when SA was labelled with Alexa-660 (Molecular Probes) and the binding experiment repeated, the energy transfer resulted in a clear decrease of the Alexa-633 lifetime, providing proof of concept for the use of similar systems in fluorescence-lifetime detection.

Conclusions and future prospects

Both techniques described in this article provide elegant approaches to detecting fluorescence lifetimes or lifetime-discriminated measurements for HTS and/or uHTS. However, we must highlight that a direct comparison of the two applications using the same assay systems was not possible as they require fluorophores with different lifetimes. Moreover, the excitation sources of the two instruments precluded measurements at the same wavelength. As both of the instruments used for the experiments discussed in this review were prototypes, we cannot at present comment on manufacturer's intentions as to their production, availability and price. Therefore, the relative merits of each approach will be discussed separately and not in direct comparison.

The different methodology, and emphasis of development of these systems highlights the general difference between conventional (i.e. macroscopic, plate reader-based) versus confocal measurements[2]. In FLARe, the system uses phase modulation techniques to discriminate and characterize the 'true' analyte fluorescence signal from background signals. The major prerequisite of this is that these two signals are of markedly different lifetime, which effectively eliminates any advantage of this approach for most conventionally used fluorophores. However, a previous report showed discrimination when fluorescein and rhodamine labels were used[28]. This is a very significant drawback, as the restricted range of dyes that are suitable for use in FLARe are fluorophores of low brightness and low labelling efficiency. Therefore, for this approach to gain broad utility in HTS, a new set of dye reagents will probably be required. In addition, the miniaturization potential of FLARe (e.g. for 1536-well plates) is unknown as yet. Low-volume 384-well conventional microplates were used for the experiments discussed here. The default read time on the FLARe instrument is 0.1 sec well^{-1}, which is compatible with uHTS throughput. However, the data presented here was collected at 0.5 sec well^{-1} to increase data quality.

By contrast, the cFLA technique is an extension of the range of confocal detection methods developed over the past few years[2,8,11]. This approach takes advantage of the confocal optical setups developed for single molecule detection techniques, which exhibit high signal to background discrimination in measurements of fluorescent tracers. Therefore, as in all such confocal methods, background signals are less of an issue than in conventional (macroscopic) plate reader systems. The cFLA approach is therefore based purely upon the characterization of tracer lifetime(s) using a straightforward time-domain single photon counting system. Moreover, the laser pulse frequency used in cFLA is designed to work well in the lifetime range commonly observed for organic dyes (i.e. <5 nsec). This opens up a wide range of possibilities for lifetime-based assays. In the examples shown here, the effects of tracer-conjugate environment on τ_f, when bioactive ligands bind to their respective receptors was exploited to construct cFLA assays. This approach has been successful in most cases that we have tested so far. The two examples shown here utilized Cy5. For this dye, conformational constraints upon ligand binding appear to result in a general lengthening of τ_f that is almost independent of the biological system being tested. Moreover, this effect is clearly not restricted to Cy5 as we have also observed effects on τ_f upon binding of a number of diverse ligand types conjugated with dyes excitable at 633 nm (e.g. MR121, MR200, Dy630; S. Turconi, unpublished results).

In addition to the detection of environmental effects upon dye conjugated biomolecules as they undergo their normal reactions, the cFLA technique has potential for use in sensing FRET processes. Currently, FRET can only be used routinely in cases where there are very large resultant changes in donor intensity (e.g. quenched peptide substrates). This imposes the constraint that the donor and acceptor pair must be in close proximity (i.e. within R_0, which is typically ~50 Å)[1]. As the precision with which cFLA appears to be able to determine lifetimes is very high (a 10–20% change is reliably detectable), and the effect upon donor lifetime is a direct and quantifiable measure of energy transfer efficiency, it is probable that this technique could significantly extend the precision and distance range of FRET measurements. This could include protein–protein interactions (e.g. binding of nuclear hormone receptors to their co-activator or co-repressor proteins)[17], or even to cell-based FRET measurement (e.g. ion-channel function)[33], as these interactions would bring the fluorophores within the R_0 distance for FRET.

Like other confocal methods, cFLA is ideally suited to the miniaturization requirements of uHTS because the signal output is independent of assay volume. The compound interference data presented here were collected at 1 µl well^{-1}, and integrated systems to assemble and perform uHTS assays in 1 µl volumes are now routinely implemented (Ashman, S., Approaches to miniaturised ultra-high throughput screening: confocal versus conventional homogeneous fluorescence assays. *IBC Screentech 2001 conference on High Throughput Screening*, 13–15 March 2001, San Diego, CA, USA; Keighley, W., Making the data work harder: real life examples from FCS. *IBC Screentech 2001 conference on High Throughput Screening*, 13–15 March 2001, San Diego, CA, USA). The high precision of lifetime measurements also enables read times of less than 0.8 sec well^{-1} (see Fig. 4c), which is required to reach a throughput of 100,000 assays day^{-1} (on a single instrument).

cFLA provides an ideal complement to the existing array of techniques that can be performed on such systems. The FIDA technique provides a confocal method for analytical determination of molecular brightness changes, and because lifetime changes are linked to brightness, these two techniques could be seen as overlapping. In reality, the converse is true, because FIDA requires brightness changes of 1.5–2.0-fold in order to work effectively[2,12], whereas cFLA appears to require far smaller changes in τ_f for construction

of robust assays. In contrast to FIDA and FCS, cFLA is not based on the analysis of fluorescence fluctuations, which imposes upper limits on the concentration of the tracer concentration (<50 nM) and can therefore be used in cases of low affinity interactions.

Acknowledgements

Both the FLARe and the cFLA instruments were prototypes and were made accessible to us via respective collaborative research agreements with LJL BioSystems (now Molecular Devices) and Evotec Biosystems (now Evotec OAI). We would particularly like to acknowledge Todd French and Michael Helms of LJL, and Leif Brand and Christian Eggeling of Evotec for excellent technical support. Furthermore, we would like to thank Ewald Terpetschinig and Jiyan Chen for the supply of the FOR fluorophore and FOR-labelled anti-pY antibody. Finally, invaluable theoretical, intellectual and managerial support came from Douglas Modlin, John Owicki and William Burton (LJL BioSystems), and Tim Jessen, Karsten Gall and Stefan Marose (Evotec Biosystems).

References

1 Pope, A.J. *et al.* (1999) Homogeneous fluorescence readouts for miniaturised high-throughput screening: theory and practice. *Drug Discov. Today* 4, 350–362

2 Haupts, U.M. *et al.* (2000) Macroscopic versus microscopic fluorescence techniques in (ultra)-high throughput screening. *Drug Discov. Today* 5 (Suppl.), 3–9

3 Sundberg, S.A. (2000) High-throughput and ultra-high-throughput screening: solution- and cell-based approaches. *Curr. Opin. Biotech.* 11, 47–53

4 Owicki, J. (2000) Fluorescence polarisation and anisotropy in high throughput screening; perspectives and primer. *J. Biomol. Screening* 4, 67–73

5 Pope, A.J. (1999) LANCE™ vs HTRF® or visa versa. *J. Biomol. Screening* 4, 301–302

6 Hemmilä, I. and Webb, S. (1997) Time-resolved fluorometry: an overview of the labels and core technologies for drug screening applications. *Drug Discov. Today* 2, 373–381

7 Kolb, A. *et al.* (1997) Homogeneous, time-resolved fluorescence method for drug discovery. In *High Throughput Screening* (Devlin, J.P., ed.), pp. 345–360, Marcel Dekker

8 Moore, K.J. *et al.* (1999) Single molecule detection technologies in miniaturised high throughput screening *J. Biomol. Screening* 4, 335–353

9 Riegler, R. (1995) Fluorescence correlations, single molecule detection and large number screening. Applications in Biotechnology. *J. Biotechnol.* 41, 177–186

10 Eigen, M and Rigler, R. (1994) Sorting single molecules: application to diagnostics and evolutionary biology. *Proc. Natl. Acad. Sci. U. S. A.* 91, 5740–5747

11 Kask, P. *et al.* (1999) Fluorescence intensity distribution analysis and its application in biomolecular detection technology. *Proc. Natl. Acad. Sci. U. S. A.* 96, 13756–13761

12 Rüdiger, M. *et al.* (2001) Single molecule detection technologies in miniaturised high throughput screening: binding assays for G-protein coupled receptors using fluorescence intensity distribution analysis and fluorescence anisotropy. *J. Biomol. Screening* 6, 29–37

13 Hemmilä, I. (1999) LANCE™; homogeneous assay platform for HTS. *J. Biomol. Screening* 4, 303–307

14 Mathis, G. (1999) HTRF⟩ Technology. *J. Biomol. Screening* 4, 309–313

15 Earnshaw, D.L. *et al.* (1999) Time-resolved fluorescence energy transfer DNA helicase assays for high throughput screening. *J. Biomol. Screening* 4, 239–248

16 Moore, K.J. *et al.* (1999) A homogeneous 384-well high throughput screen for novel tumour necrosis factor receptor:ligand interactions using time-resolved spectroscopy. *J. Biomol. Screening* 4, 205–214

17 Zhou, G. *et al.* (1999) Nuclear hormone receptors have distinct affinities for coactivators; characterisation by fluorescence resonance energy transfer. *Mol. Endocrinol.* 12, 1594–1604

18 Kane, S.A. *et al.* (2000) Development of a binding assay for p53/HDM by using homogeneous time-resolved fluorescence. *Anal. Biochem.* 278, 29–38

19 Cummings, R.T. *et al.* (1999) Use of a phosphotyrosine-antibody pair as a general detection method in homogeneous time-resolved fluorescence: application to human immunodeficiency viral protease. *Anal. Biochem.* 269, 79–93

20 Zhang, J-H. *et al.* (2000) A high-throughput homogeneous assay for reverse transcriptase using generic reagents and time-resolved fluorescence detection. *Anal. Biochem.* 281, 182–186

21 Lakowicz, J.R. (1999) *Principles of Fluorescence Spectroscopy* (2nd Edn), Kluwer Academic, New York

22 Lakowicz, J.R. (1995) Fluorescence spectroscopy of biomolecules. In *Encyclopaedia Of Molecular Biology And Molecular Medicine* (Meyers, R.A., ed.), UCH Publishers

23 Jameson, D.M. and Hazelett, T.L. (1991) Time-resolved fluorescence in biology and biochemistry. In *Biophysical and Biochemical Aspects of Fluorescence Spectroscopy* (Dewey, T.G., ed.), pp. 105–133, Plenum Press

24 Lakowicz, J.R. *et al.* (1987) Correction for contaminant fluorescence in frequency-domain fluorometry. *Anal. Biochem.* 160, 471–479

25 French, T. *et al.* (1998) Fluorescence lifetime technologies for high throughput screening. *Proc. SPIE* 3259, 209–218

26 French, T. *et al.* (1999) A time-resolved fluorimeter for high-throughput screening. *Proc. SPIE* 3603, 272–280

27 Caspar, J.V. *et al.* (1982) Application of the energy gap law to the decay of charge-transfer excited states. *J. Am. Chem. Soc.* 104, 630–632

28 Helms, M.K. and French, T. (2000) Time-resolved fluorescence measurements of actin phalloidin interactions. *Proc. SPIE* 3926, 158–165

29 O'Connor, D.V. and Phillips, D. (1984) *Time Correlated Single Photon Timing*, Academic Press

30 Schaffer, J. *et al.* (1999) Identification of single molecules in aqueous solution by time-resolved fluorescence anisotropy. *J. Phys. Chem.* 103, 331–336

31 Becker, W. *et al.* (1999) Time-resolved detection and identification of single analyte molecules in microcapillaries by time-correlated single-photon counting (TCSPC). *Rev. Sci. Instru.* 70, 1835–1841

32 Zhang, J.H. *et al.* (1999) A simple statistical parameter for use in evaluation and validation of high-throughput screening assays. *J. Biomol. Screening* 4, 67–73

33 Gonzales, J.E. *et al.* (1999) Cell-based assays and instrumentation for screening ion-channel targets. *Drug Discov. Today* 4, 431–439